Using Vegetation Management and LiDAR-Derived Tree Height Data to Improve Outage Predictions for Electric Utilities

D.W. Wanik[1]; J.R. Parent[2]; E.N. Anagnostou[1]; B.M. Hartman[3]

[1] Department of Civil and Environmental Engineering, University of Connecticut

[2] Department of Natural Resources and the Environment, University of Connecticut

[3] Department of Statistics, Brigham Young University

Submitted in October 2016 to:

Electric Power Systems Research

Abstract

We have generated a light detection and ranging (LiDAR) data product that provides a 1-meter resolution measurement of vegetation that is tall enough to strike overhead distribution powerlines, called “ProxPix”. These data, along with other vegetation management (e.g. tree trimming) and infrastructure data were evaluated for their improvement an outage prediction model over Eastern Connecticut during Hurricane Sandy. We found that models inputted with infrastructure, vegetation management, ProxPix, performed better than simpler models; and that the model forced with utility infrastructure and ProxPix had the best overall performance. The ProxPix data created for this study have application to other research topics such as prioritizing areas for vegetation management near utilities and providing data on potential tree threats to roads or railways.

Keywords: Electric distribution network, severe weather, outage prediction model, vegetation management, resilience, LiDAR

1. INTRODUCTION

Connecticut has been subjected to prolonged power outages due to damage caused primarily by the interaction of trees and overhead power lines during extraordinary storms (i.e. Storm Irene and the October nor'easter in 2011, and Hurricane Sandy in 2012). Hurricane Sandy was especially impactful to Eversource Energy (formerly Connecticut Light & Power), with >500,000 customers without power and >15,000 outages (defined as individual locations requiring the manual intervention of a utility restoration crew for repair) caused mostly by branches or entire trees falling onto the overhead lines (1). Contributing to these high storm-related outages, Connecticut has the highest wildland-urban interface in the United States (2) with a majority of residents living under a rural or urban tree canopy.

Trees provide a host of benefits including: habitat for wildlife (3), shade that moderates temperatures (4), and aesthetic benefits (5). Electric utility companies are tasked (6) with managing these trees surrounding overhead lines to maintain acceptable reliability for customers (e.g. limiting the number of interruptions and duration of outages). The management of trees and other flora around overhead lines is known as vegetation management (VM); a multi-faceted program of managing trees by trimming above, below and on the side of overhead lines; and the management of vines and shrubs.

Despite the influence of vegetation management on electric reliability during storms, there is limited information available on how VM affects distribution networks. Among these studies, (7) showed that increasing trimming on distribution circuits could lead to decreased outages on the Duke Power system in the Carolinas. Although multiple VM trimming strategies exist (e.g. trim overhead lines every 2 – 7 years), (8) showed that an optimized vegetation

management program as a function of utility cost and customer cost could yield an improvement in reliability (4 – 6%) and a reduction in total cost (9%). Other researchers (9) have investigated including VM data and other weather and geographic data into outage prediction models and found that the data could help the accuracy of these models.

Utilities typically track where VM has occurred on the overhead lines in a geographic information system. Airborne Light Detection And Ranging (LiDAR) data complement VM data by making it possible to develop accurate models of tree heights and locations over large areas. Airborne LiDAR data have been used for more than a decade to model the heights of forest canopies (10). Canopy height models (CHM) estimate forest canopy height at any given location and make it possible to identify trees that are within striking distance of power lines. The identification of these risk trees provides a direct physical basis for outage prediction models to better incorporate the environmental conditions surrounding overhead power lines.

The objective of this paper is to evaluate the available data on trees and infrastructure for their effect on improving hurricane outage model predictions. Specifically, we compare models incorporating these datasets to more traditional models that incorporate only limited environmental data. Given the temporal and spatial constraints of the data, we focus our paper exclusively on damages during Hurricane Sandy (2012) in eastern Connecticut. This paper is divided into six additional sections: Section 2 describes the study area; Section 3 describes the data used in more detail; Section 4 describes the methodology and error metrics; Section 5 presents the results; Section 6 discusses the results; and Section 7 presents the conclusion and future areas of research.

2. STUDY AREA

The study area is focused on eastern Connecticut (Figure 1) due to the availability of LiDAR data over the region. Eastern Connecticut has a diverse landscape with a lowland coastal southern region and a hilly northern region encompassing the Thames River valley. Population is most heavily concentrated along the shoreline and along the Thames River valley. Eversource Energy-Connecticut delivers power to nearly every town in eastern Connecticut except for three which are served by municipal utilities.

3. DATA

The data used in this study (described below) were aggregated using a grid with 0.5x0.5 km cell sizes; representing a total of 9,000 grid cells covering the study area. All datasets were averaged within each grid cell. Weather simulation data were processed at 2 km spatial resolution using the Weather Research and Forecasting (WRF) model (11), while all other explanatory data were processed at the 0.5 km grid resolution. For this study, we used the weather simulation and land cover data for Hurricane Sandy as described in (RW.ERROR - Unable to find reference:256) - see this article for a full description of the simulation methodology and validation of winds. Examples of variables from the weather simulation include the maximum gust and wind at 10 m, the total accumulated precipitation, and the duration of wind at 10 m above specific thresholds (i.e. 9, 13, and 18 m/s). To join the 2 km weather data to the 0.5 km aggregated data, the centroid of each 0.5 km grid cell was joined to the nearest 2 km centroid and assigned the corresponding data. See Table I for a description of all variables included in the model.

3.1 Utility Infrastructure

We considered attributes of the conductors related to their circuit material (e.g. bare or covered) and designation (e.g. backbone or lateral) to make the model more physically-meaningful. Conductor material was deemed important because the overhead lines suffer from different types of outages (i.e. incidental touching of trees for bare conductors, destruction of conductors for bare and covered conductors). Circuit designation was included because backbone circuits typically serve many more businesses and essential town functions (e.g. police, fire, ambulance) than lateral circuits, and are expected to be more resilient due to enhanced VM activities from 1994 - 2007 (Personal Communication, Sean Redding, Eversource Energy).

3.2 Vegetation Management

Using vegetation management annual planning data for years 2009 through 2012, we calculated the percentages of overhead lines that received SMT and ETT treatment as a function of conductor material and circuit designation for a given year in each 0.5 x 0.5 km grid cell. A linear decay function (Equation 1) was applied to the SMT to express the diminishing benefit of such treatment as time passes due to regrowth. A cumulative function (Equation 2) was applied to ETT because the benefit of such trimming activities are thought to be longer lasting and more effective than SMT (Personal Communication, Sean Redding, Eversource Energy).

In summary, for each conductor material and circuit designation, we calculate the SMT or ETT value per grid cell as follows:

$$SMT\ Value = \sum_{j=2009}^{2012} SMT_j \cdot r \cdot (2012 - j) \quad (1)$$

$$ETT\ Value = \sum_{j=2009}^{2012} ETT_j \quad (2)$$

In the above two equations; SMT and ETT refer to the percentage of lines that were trimmed during the year, respectively; the year is j; the decay rate (25% per year) is *r*. Note that Sandy occurred in 2012 and the earliest date for which trim data were available is 2009. Figure 2 shows the distribution of trimming by type (ETT vs. SMT) across the entire study area from 2009 - 2012. Refer to Table I for a summary of the different variables related to vegetation management.

Note that the Enhanced Tree Trimming (ETT) specification during 2009 – 2012 along the roadside differed for backbone and lateral circuits. Regarding ETT roadside clearance for lateral circuits, the clearance zone from the conductor was 8 feet to the side, 20 feet overhead and cut brush flat to the ground; for backbone circuits, the clearance zone from the conductor was clear overhead, 8 feet to the side, and brush was cut to the ground. Exceptions to these specifications could be granted in some cases at the request of a tree owner or town (Personal Communication, Sean Redding, Eversource Energy). Comparatively, the Standard Maintenance Trimming (SMT) specification during 2009 -2012 was less intensive. The roadside SMT clearance for lateral circuits was a minimum of 8 feet to the side, 15 feet overhead, 10 feet below clearance within reach of a 55 foot lift unit; for backbone circuits, trimming must re-clear to previous overhead clearances within reach of a 70 foot lift unit.

3.3 LiDAR-Derived Tree Height Information

Airborne LiDAR data were acquired for nearly 4600 km^2 in eastern Connecticut from November 3 – December 11, 2010 (12) (Figure 1). The data were collected with a Leica ALS60 Airborne Laser Scanner at an altitude of approximately 2,000 meters above ground level. At this altitude, the ALS60's beam divergence of 0.22 millirads creates a footprint of roughly 44 cm on

the ground. The scanner's pulse rate was 117.9 kHz and the pulse wavelength was 1064 nm. The flight line overlap was 50% and the data provider eliminated data between the geometrically usable portions of the swaths. The maximum scan angle of the sensor was 16.5^0 from nadir and it recorded up to 4 returns per laser pulse. The dataset has an overall density of 1.56 returns / m^2 with a maximum point spacing of 0.7 meters, excluding water bodies. The horizontal accuracy of the dataset is equal to or better than 1 meter RMSE. The project's principle contractor processed the LiDAR data to create a bare-earth digital elevation model (DEM), at a 1-meter resolution, with building features removed. Dewberry (12) evaluated the accuracy of the DEM using 62 surveyed ground control points distributed through non-vegetated, grass, and forested terrains. The vertical RMSE for the DEM, based on ground control points, was estimated at 5 cm in non-vegetated terrain, 17 cm for grassy terrain, and 21 cm in forest terrain. The primary purpose of the LiDAR dataset was to develop the bare-earth DEM for use in conservation planning, floodplain mapping, dam safety assessments, and hydrological modeling (12).

3.3.1 Canopy Height Model

A canopy height model, based on airborne LiDAR, was created following the methods described in (13). The CHM was created by subtracting the bare-earth DEM, created by Dewberry (12), from a digital surface model (DSM) that we created from the LiDAR data. The DSM corresponded to the maximum elevations in the tree canopy and was aligned to the DEM grid and had the same 1-meter resolution. The cell values for the DSM were determined by taking the maximum of all non-ground first-return points within a given cell. Because the overall density of the LiDAR dataset was 1.56 returns / m^2, the majority of non-water pixels in the DSM grid contained at least one first-return point. The first-returns were filtered to remove points that obviously did not correspond to features on the earth's surface (e.g. large birds in flight). These

anomalous points were identified by comparing each first-return to all points within a 2.5 meter radius. Points were discarded if they were more than 30 meters taller than any other points within the neighborhood. We selected the 30-meter threshold because it approximates the upper limit of canopy heights in northeastern forests and thus it represented a reasonable maximum elevation difference for points along forest gaps and edges. Considering the point spacing of our airborne LiDAR data, we assumed that continuous data gaps larger than 3 meters in radius were likely to correspond to water, which tends to absorb LiDAR energy (14). The bare-earth DEM values were assigned to the cells in these larger data gaps that were presumed to correspond to water bodies. A test of 52 1x1 km sample areas showed that only 12.9%, on average (std. dev. = 3.4), of the areas consisted of data gaps for which there was no first-return data. More than 91% of these gaps were less than 1 meter in radius; approximately 7% of the gaps were 1-2 meters in radius; and approximately 1% of the gaps were 2-3 meters in radius. Thus, we interpolated the values for cells in the DSM data gaps, smaller than 3 meters in radius, by taking the median of the known values in the cells' eight nearest neighbors. Cells with fewer than three known nearest neighbors were filled using a 2^{nd} or 3^{rd} interpolation pass.

3.3.2 Proximal Tree Pixels

Previous studies have suggested that mapping of individual tree crowns requires LiDAR data with a spatial resolution of at least 4-8 pts / m^2 (15, 16). Because the resolution of our data (<2 pts/m^2) was insufficient for mapping crowns, we used "proximity tree pixels" as a surrogate for risk trees. We define proximity tree pixels (ProxPix) as 1 m pixels in a canopy height model (CHM) that are tall enough and close enough to contact a power line in the event of a whole or partial tree failure. Multiple ProxPix can correspond to a single tree; however, intuitively, we expected a high correlation between the number of ProxPix and number of trees corresponding to

those ProxPix. ProxPix were identified from the canopy height model as pixels with a height larger than the distance from the pixel at ground-level to a point 10 m above ground at the location of the nearest power line (Figure 3). The ground-level for a pixel was determined from the bare-earth DEM; 10 meters was assumed to be the height of the primary lines above ground level.

The power line dataset had a median horizontal position error of 11.8 meters (std. dev. = 9.9m). Therefore, we created a 15 m buffer around the reported power line locations and mapped ProxPix treating the buffer zone as the power line. ProxPix were extracted throughout the study area (Figure 1) and aggregated into counts for the 0.5 km grid. The counts were then normalized by total overhead line length (resulting in ProxPix/km) for use in the models.

4 METHODOLOGY

4.1 Model Forcing Complexities

To ensure that predictors were not contributing unnecessary complexity in the model structure, five model forcing complexities (Table I) were evaluated to investigate the added value to the outage prediction model of incorporating: (a) vegetation management, (b) the LiDAR-derived proximal tree pixel dataset and (c) detailed infrastructure. The baseline model (Model 1) was used for comparison to the more complex models and consisted of a full set of weather variables, land cover, and the count of isolating devices per grid cell to represent the overhead infrastructure. This model is most similar to those in (RW.ERROR - Unable to find reference:256) and (17). Model 2 builds upon the baseline model with the addition of the circuit material and designation data, as well as land cover data. Model 3 builds upon Model 2 with the addition of vegetation management data. Model 4 also builds upon Model 2 with the addition of

ProxPix data. Model 5 is the most comprehensive, including detailed infrastructure, vegetation management, and ProxPix data. To compare the benefit of ProxPix and land cover, Models 1 – 3 used land cover data to represent the local tree conditions while Models 4 and 5 used ProxPix as an alternative to land cover.

4.2 Description of Random Forest Algorithm

The statistical software program R (18) was used to complete all modeling and analyses. The R package "randomForest" (19) was used to predict the binary response variable. We selected the random forest model due to its efficiency and satisfactory performance in previous literature that predicted hurricane damages (RW.ERROR - Unable to find reference:256) and outages (9). Random forest (20) is an extension of the classification and regression tree ("decision tree") model (21); whereas a decision tree makes a series of logical "if-then" statements from a single pass through the training partition, the random forest uses a random subset of the training data and a random subset of explanatory variables to fit multiple decision trees (20). The predictions from all of the decision trees are referred to as the "forest" – the average of the forest predictions are used as the final prediction.

4.3 Binary Response Variable and Model Evaluation

Outages are defined as locations that require a restoration crew to manually intervene to restore power. Of the 9,000 grid cell in the 0.5 km spatial domain, 1,320 had one outage, 440 had more than 1 outage, and no grid cell had more than eight outages. Because of this distribution, we used binary response models with a balanced sampling approach to investigate the accuracy of outage predictions. An indicator of "1" was assigned if an outage occurred in the grid cell, otherwise a "0" was assigned. Grid cells without an outage (n=7,240) are referred to as the majority class, grid cells with an outage (n=1,760) are referred to as the minority class. The

balanced random forest (BRF) algorithm proposed by (22) consists of down-sampling the majority class to learn from imbalanced by fitting a single model. In order to maximize the information of the majority class, we repeated the BRF algorithm 10,000 times and compared the error metrics for each iteration. This approach resulted in a distribution of the error metrics for each of the five model complexities we investigated. For each of the 10,000 iterations, the model complexity with the most improved error metrics was selected as the "winner". The frequency of how many times each model was selected the "winner", based on the error metrics, is summarized in Table II.

4.4 Error Metrics

The R package "SDMTools" (23) was used to calculate various contingency table metrics to describe the model performance more completely. Specifically, we used the following metrics for model comparison: area under the curve (AUC), false omission rate (FOR), true positive rate (TPR), true negative rate (TNR), proportion correct (PC), and Cohen's kappa (K). For the following equations (Eq. 4 through 7); TP (true positive) refers to the counts of true positives; TN (true negative) refers to the counts of true negatives; FP (false positives) refers to the counts of false positives; and FN (false negatives) refers to the counts of false negatives.

$$FOR = \frac{FN}{FN+TN} \qquad (4)$$

$$TPR = \frac{TP}{TP+FN} \qquad (5)$$

$$TNR = \frac{TN}{TN+FP} \qquad (6)$$

$$PC = \frac{TP+TN}{TP+TN+FP+FN} \quad (7)$$

$$\mathrm{K} = \frac{2\left((TP*TN)-(FP*FN)\right)}{(TP+FN)(FN+TN)+(TP+FP)(FP+TN)} \quad (8)$$

Each of the metrics we evaluated has desirable properties that describe the model performance. The area under the Receiver Operating Characteristic curve (AUC) is an accuracy metric that shows the model discrimination (the ability to correctly identify true negatives positives); an AUC of 1 represents a perfect prediction whereas an AUC of 0.5 or less represents a test that is no better than chance. The false omission rate (Equation 4) is the proportion of false negatives given the test outcome was negative; a FOR of 1 indicates that all predictions for negatives were false whereas a FOR of 0 indicates that there were no false negative. The true positive rate (TPR), also known as sensitivity, is how many times TP was correctly predicted given a positive reading; a TPR of 1 indicates a model is perfect at predicting true positives, a TPR of 0 indicates a model that is incapable of predicting true positives. The true negative rate (TNR), also known as specificity, is a measure of how many times true negatives are actually predicted; a TNR of 1 indicates a model is perfect at predicting where damage will not occur, a TNR of 0 indicates a model that fails to predict where outages will not occur. The proportion correct (PC) is a measure of how many observations are correctly identified; a PC of 1 indicates a perfect predictor, a PC of 0 indicates a predictor that fails to predict where actual outages occur. Cohen's kappa statistic (K), also known as Heidke Skill Score, is a measure of agreement between categorical variables based on the proportion correct. A K of 1 indicates a perfect prediction, and zero or negative values can happen when forecasts are equal to or worse than the reference.

5 RESULTS

The error metrics of Model 1 were used as baseline to compare subsequent models with increasingly complex model forcings (Models 2 through 5). As previously mentioned, the validation strategy used repeated balanced sampling (RBS) with 10,000 iterations to select which model performed the best for each of the five models . The frequency of how many times each model was selected the "winner", based on the error metrics, is summarized in Table II. Models 2 – 5 were selected more frequently for most error metrics than the baseline model (Model 1). Model 4 was the most frequently selected for AUC, TNR, PC, and K error metrics, while Model 5 was the most frequently selected for TPR and FOR. Although Model 5 was selected most frequently for these two metrics, Model 4 was the second most selected model. Under the validation strategy we used to compare the five model forcing complexities, Model 4 proved to be the best model for the following error metrics: AUC, TNR, PC and K (Tables 2 and 3). Although Model 4 was "better" (more frequently selected) than Model 1 for TNR, it was only marginally better, which may indicate that a simpler model forcing complexity may yield better predictions of the true negatives. The next best model was Model 5, the most complex model, and was most frequently selected for two error metrics (FOR and TPR). To compare model performance, each model was ranked (1 – 5) across all error metrics based on frequency (where 1 is considered the most frequent and 5 is least frequent). The average of these individual error metric rankings was computed to select the best overall model. Overall, Model 4 was the best model followed by Models 5, 3 and 2 (Table 4). From a physical perspective, the superiority of Model 4 is attributed to the model forcing complexity that included ProxPix, which in turn gave the best representation of local tree risk and more accurate outage predictions (this will be discussed further in Section 7).

The kernel density plots in Figure 5 show the improved performance of Model 4 compared to the Model 1 (baseline model) for all error metrics. The value of AUC, TPR, TNR and PC ranged between 0.58 - 0.72; while K values varied between 0.19 – 0.43. The maximum improvement for each metric between Models 1 and 4 was 6% for AUC, 5% for FOR, 9% for TPR, 7% for TNR, 6% for PC, and 13% for K. However, the average improvement of Model 4 compared to Model 1 was 1% for AUC, 2% for FOR, 2% for TPR, 1% for PC, 2% for K and no improvement on average for TNR. Figure 5 shows a clear separation between the kernel density plots for each category except for TNR where the distribution of values nearly overlapped.

We now focus on the results of Model 5, as it includes the interaction of all variables of interest related to weather, infrastructure and tree conditions. The variable importance plot in Figure 6 details the degree to which a specific covariate contributed to Model 5 as measured by the mean decrease in the Gini coefficient. The three most important variables were the total length of overhead lines, the sum of the assets, and the ProxPix normalized by overhead line length. Also among the top ten most important variables were the storm accumulated precipitation, the mean and maximum gust, and the precipitation rate. Figure 7 shows partial dependence plots, which details the dependence between the response variable and a specific covariate, marginalizing over the values of all other variables. The covariate of interest is plotted on the x axis, while the y axis provides the response variable (in this case, it is the logit of the predicted outages). Variables that had a contribution to decreased predicted outages included the total overhead length and sum of assets. In contrast, increased mean gust and wind at 10 m contributed to increased predicted outages. On backbone lines, ETT and SMT on backbone bare and covered lines showed a decrease in predicted outages, while lateral lines have a mixed response depending on conductor material and circuit type.

6 DISCUSSION

We have evaluated the error metrics of five model forcing complexities related to infrastructure and local tree conditions, and investigated the improvement of each complexity in an outage prediction model with a binary target variable. The inclusion of additional variables related to the distribution network infrastructure and local tree risk data (ProxPix) resulted in improved error metrics and model performance. A comparison of Model 1 and Model 2 shows that the model with additional infrastructure data on circuit material and designation performed better than the reduced infrastructure model. A comparison of Model 2 and Model 3 suggests that VM data and infrastructure data can be a decent substitute for tree canopy height data. Models that combine tree height and detailed infrastructure data would yield the best performance.

Our results are consistent with other papers in the literature that show that incorporating additional data on infrastructure and environmental conditions can yield at improved outage predictions (read below for further explanation). In particular, this current study supports our previous study (RW.ERROR - Unable to find reference:256), which showed that including additional information on land cover and infrastructure can be used to improve the spatial accuracy of outage predictions during hurricanes.

Many recent outage modeling papers that use a grid-averaged approach predict the count of outages per grid cell rather than modeling the probability of an outage occurring (9, 24-26). Despite difference in response variable type, grid cell resolution, geographic region, storms and model forcing, we can still draw comparisons to other papers on the influence of certain variables contributing to the predicted outages. Nateghi et al. (9) presented partial dependence plots that demonstrate how VM contributed to increased predicted hurricane outages in two Gulf

region states, and also showed that the mean absolute error per grid cell increased 43 – 53% when outage models were fit without VM data. We build on these results and show that VM can contribute to either an increase or decrease in predicted outages depending on the infrastructure attributes. Specifically, the increase of ETT and SMT on backbone lines contributes to lower predicted outages regardless of conductor material; while the pattern varied by treatment, conductor material and circuit designation for lateral lines (Figure 7).

The benefits of VM during non-storm conditions in the Duke Power System (Carolinas) was previously modeled by (7), who showed that going from a four year to a three year trimming cycle would eliminate 0.9 outages per circuit over a 43 month period. We are unable to make the conclusion that VM reduces hurricane outages because our paper is limited by a single region and storm. However, seeing change in predicted outages as a function of conductor material and circuit type is promising (Figure 7), and provides motivation to incorporate additional data on the overhead infrastructure and local tree conditions in future studies. In addition, building on the previous work by (27) who showed how storm attributes would contribute to longer restoration times, we believe ProxPix may be able to enhance outage duration predictions by providing information on local tree conditions which may be correlated with damage severity (i.e. broken wire vs. broken pole). As time progresses, we hope to extend our methodology to analyze how VM, ProxPix and infrastructure contribute to outage predictions from more frequently occurring storms (e.g. thunderstorms and nor'easters)

CONCLUSION

We have presented a study that shows that the inclusion of data related to localized tree conditions (ProxPix and vegetation management) and utility infrastructure can improve outage

prediction models with a binary response variable. We found that more complex models with vegetation management, ProxPix, and infrastructure performed better than the simple baseline model; and that the model forced with utility infrastructure and ProxPix had the best overall performance. The ProxPix data created for this study have application to other research topics such as prioritizing areas for vegetation management near utilities and providing data on potential tree threats to roads or railways. Guikema et al. (28) previously showed how an outage model calibrated with publicly available data in the Gulf region could be applied to show the impact of historic storms in different geographic regions. This approach could over- or underestimate outages as each electric utility has different utility infrastructure and vegetation conditions, which are not well represented by land cover data alone. With the use of LiDAR, the methodology in (28) could potentially benefit from the quantitative measurement of tree conditions along roadsides across all utilities and be used to enhance these models. In addition, given that the majority of overhead lines follow roadways, LiDAR-derived tree height data near utility lines could also be used for determining which roads might be most vulnerable to downed trees.

Acknowledgements: We greatly acknowledge the funding from the Electric Power Research Institute and the data from Eversource Energy. Many thanks to those who provided helpful comments to improve this manuscript.

REFERENCES

1. Connecticut Light & Power. Transmission and Distribution Reliability Performance Report. Berlin, CT: Connecticut Light & Power; 2014 Available from: http://www.dpuc.state.ct.us/DOCKCURR.NSF/60903cc7b9de44728525746b006e8ffb/027ee9c77ff179fb85257cac006627be?OpenDocument&scrollTop=0&scrollTop=1419

2. Stewart SI, Radeloff VC, Hammer RB. The Public and Wildland Fire Management: Social Science Findings for Managers. Newtown Square, PA: United States Department of Agriculture, Forest Service; 2006. Report No.: NRS-1 Available from: http://www.fs.fed.us/nrs/pubs/gtr/gtr_nrs1.pdf

3. Cadenasso ML, Pickett STA. Linking forest edge structure to edge function: Mediation of herbivore damage. J Ecol [Internet]. 2000 [cited 16 May 2016];88(1):31-44.

4. Armson D, Stringer P, Ennos AR. The effect of tree shade and grass on surface and globe temperatures in an urban area. Urban For Urban Greening [Internet]. 2012 [cited 16 May 2016];11(3):245-55.

5. Gerstenberg T, Hofmann M. Perception and preference of trees: A psychological contribution to tree species selection in urban areas. Urban For Urban Greening [Internet]. 2016 [cited 16 May 2016];15:103-11.

6. IEEE. C2-2007 National Electric Safety Code - PDF Single User Professional Edition : VuSpec (NESC). [Internet]. ; 2007 DOI: https://doi.org/10.1109/ieeestd.2006.322219

7. Guikema SD, Davidson RA, Liu H. Statistical models of the effects of tree trimming on power system outages. IEEE Trans Power Delivery [Internet]. 2006 [cited 2 September 2014];21(3):1549-57.

8. Kuntz PA, Christie RD, Venkata SS. Optimal vegetation maintenance scheduling of overhead electric power distribution systems. IEEE Trans Power Del [Internet]. 2002 [cited 21 December 2014];17(4):1164-9.

9. Nateghi R, Guikema S, Quiring SM. Power outage estimation for tropical cyclones: Improved accuracy with simpler models. Risk Anal [Internet]. 2014 [cited 22 July 2014];34(6):1069-78.

10. Lim K, Treitz P, Wulder M, St-Ongé B, Flood M. LiDAR remote sensing of forest structure. Prog Phys Geogr [Internet]. 2003 [cited 18 January 2015];27(1):88-106.

11. Skamarock, W. C. et al. A Description of the Advanced Research WRF Version 3. Boulder, Colorado: NCAR; 2008. Report No.: TN–475+STR Available from: http://www2.mmm.ucar.edu/wrf/users/docs/arw_v3.pdf

12. Dewberry. Project Report for the U.S. Corps of Engineers High Resolution LiDAR Acquisition & Processing for Portions of Connecticut. Dewberry; 2011. 77 p. Report No.: USACE Contract W912P9-10-D-053

13. Parent JR, Volin JC. Modeling forest canopy height using moderate resolution leaf-off airborne light detection and ranging (LiDAR). International Journal of Remote Sensing. 2015;Revisions pending: December 2014

14. Campbell JB. Introduction to remote sensing. Introduction to remote sensing [Internet]. 1987 [cited 18 January 2015]

15. Evans JS, Hudak AT, Faux R, Smith AMS. Discrete return lidar in natural resources: Recommendations for project planning, data processing, and deliverables. Remote Sens [Internet]. 2009 [cited 19 September 2016];1(4):776-94.

16. Laes D, Reutebuch S, McGaughey B, Maus P, Mellin T, Wilcox C, Anhold J, Finco M, Brewer K. Practical lidar acquisition considerations for forestry applications. 2008. 7 p. Report No.: RSAC-0111-BRIEF1

17. He J, Wanik DW, Hartman BM, Anagnostou EN, Astitha M, Frediani MEB. Nonparametric tree-based predictive modeling of storm outages on an electric distribution network. Risk Anal [Internet]. 2016 [cited 20 September 2016]

18. R Core Team. R: A Language and Environment for Statistical Computing. Vienna, Austria: R Foundation for Statistical Computing; 2014.

19. Liaw A, Wiener M. Classification and regression by randomForest. R News. 2002;2(3):18-22.

20. Breiman L. Random forests. Random Forests [Internet]. 2001 [cited 18 January 2015]

21. Breiman L, Friedman JH, Olshen RA, Stone CJ. Classification and Regression Trees [Internet]. 1984 [cited 22 July 2014]

22. Chen C, Liaw A, Breiman L. Using Random Forest to Learn Imbalanced Data. Department of Statistics, UC Berkeley; 2004. Report No.: 666

23. VanDerWal J, Falconi L, Januchowski LS, Storlie L. SDMTools: Species Distribution Modelling Tools: Tools for processing data associated with species distribution modelling exercises. ; 2014.

24. Han S-, Guikema SD, Quiring SM, Lee K-, Rosowsky D, Davidson RA. Estimating the spatial distribution of power outages during hurricanes in the gulf coast region. Reliab Eng Syst Saf [Internet]. 2009 [cited 22 July 2014];94(2):199-210.

25. Han S-, Guikema SD, Quiring SM. Improving the predictive accuracy of hurricane power outage forecasts using generalized additive models. Risk Analysis [Internet]. 2009 [cited 15 August 2014];29(10):1443-53.

26. Liu H, Davidson RA, Apanasovich TV. Spatial generalized linear mixed models of electric power outages due to hurricanes and ice storms. Reliab Eng Syst Saf [Internet]. 2008 [cited 22 July 2014];93(6):897-912.

27. Nateghi R, Guikema SD, Quiring SM. Forecasting hurricane-induced power outage durations. Nat Hazards [Internet]. 2014 [cited 8 February 2015];74(3):1795-811.

28. Guikema SD, Nateghi R, Quiring SM, Staid A, Reilly AC, Gao M. Predicting hurricane power outages to support storm response planning. Access, IEEE [Internet]. 2014;2:1364-73.

List of Figures

List of Tables

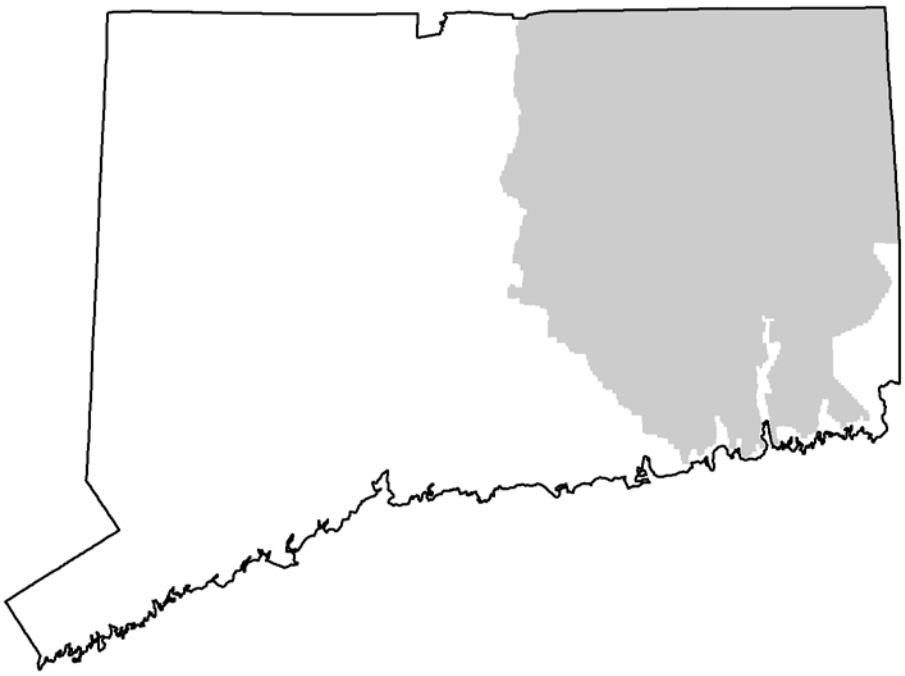

Figure 1: Distribution of the 4600 km^2 LiDAR data in eastern CT over the study area.

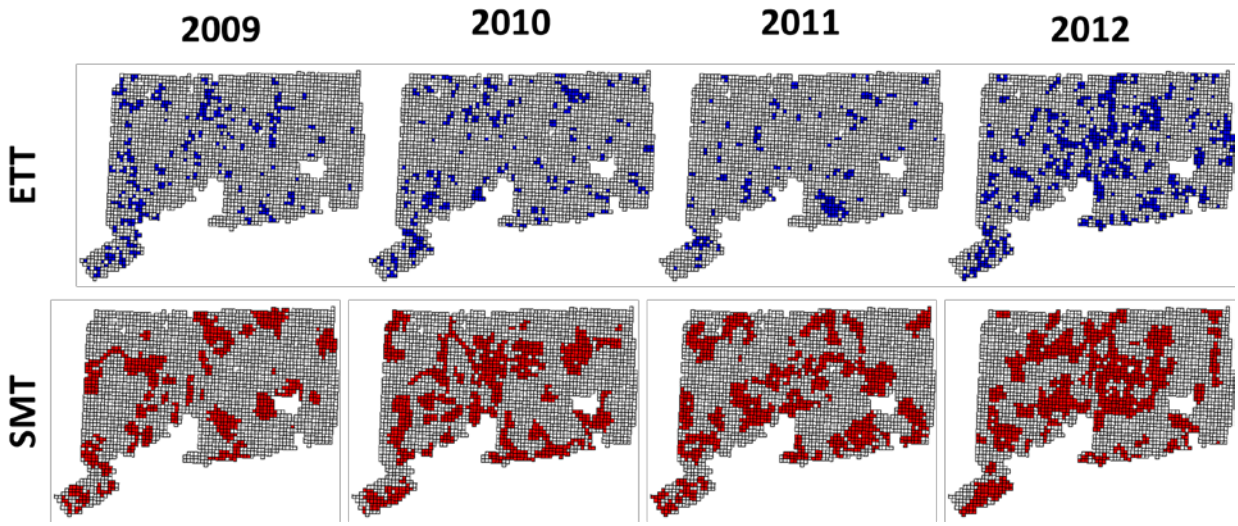

Figure 2: Comparison of grid cells across Eversource CT service territory. Grid cells with color represent that trimming occurred (does not reflect how intense the trimming was).

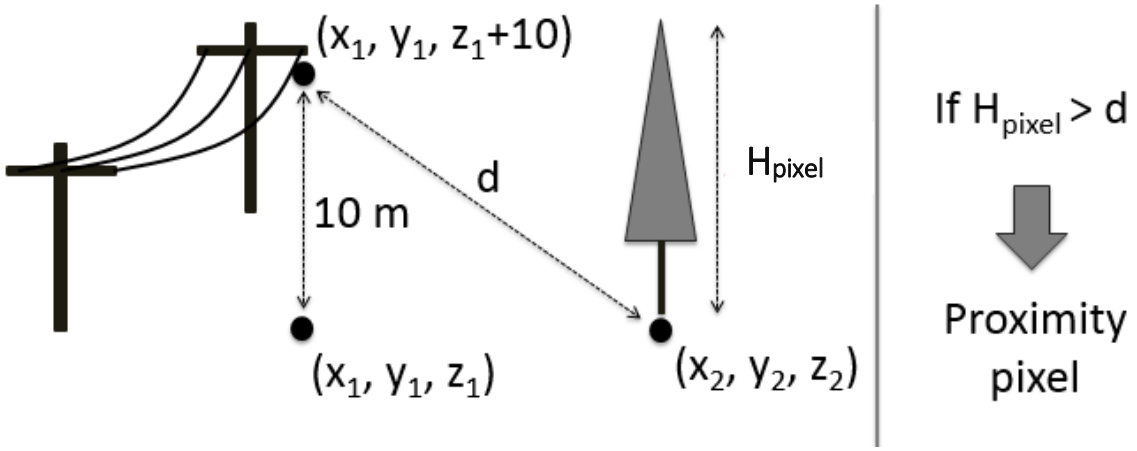

Figure 3: Identifying proximity pixels in the canopy height model based on pixel height and distance to power lines.

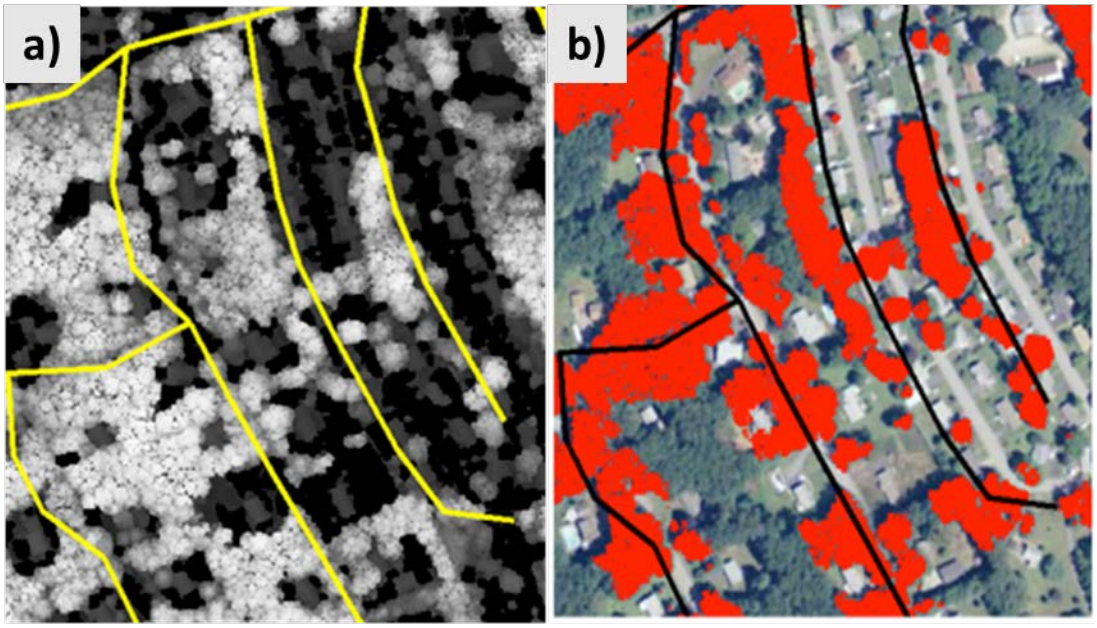

Figure 4: (a) Canopy height model with 1 m spatial resolution based on LiDAR data, lighter colors indicate taller features; (b) model of ProxPix (red) near power lines.

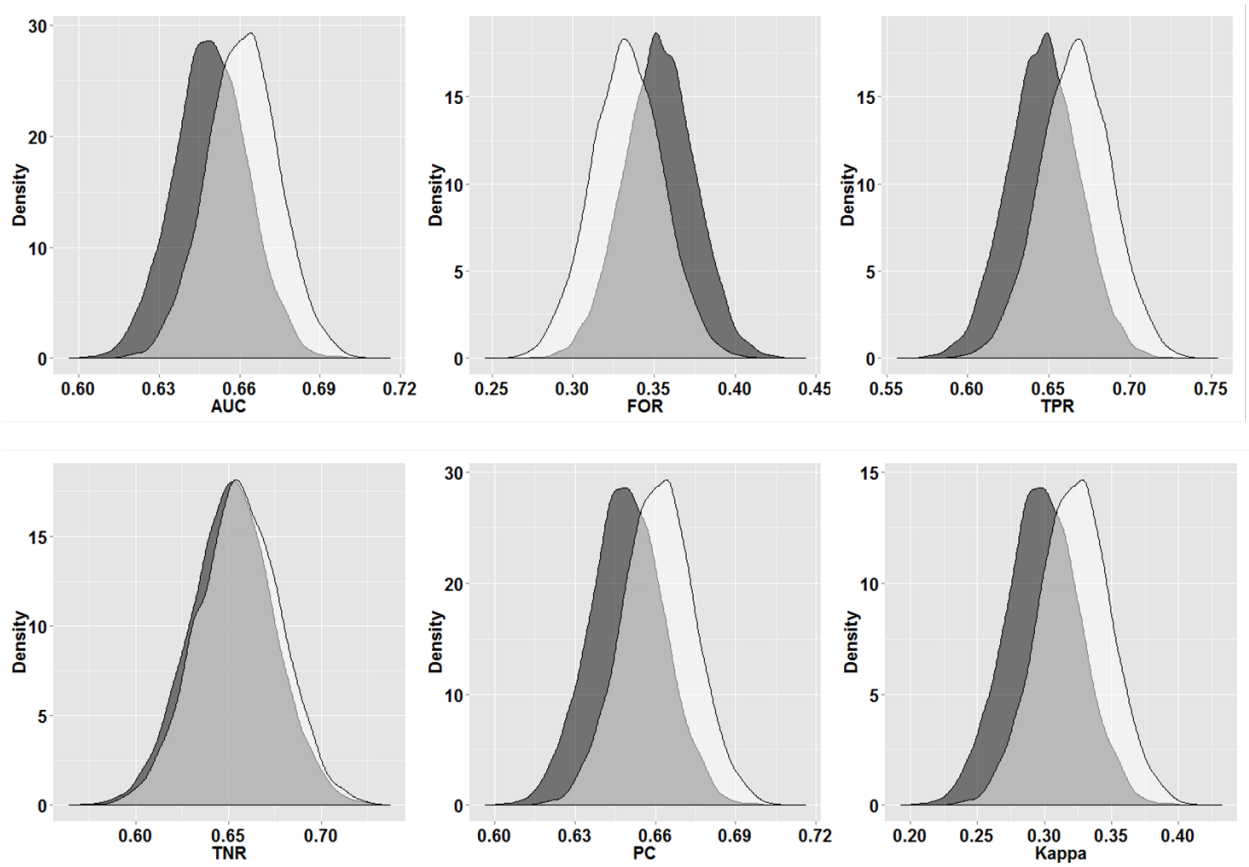

511

512 **Figure 5:** Panel plot of all contingency metrics evaluated (dark gray = Model 1, white = Model

513 4, light gray = overlap of Model 1 and Model 4).

514

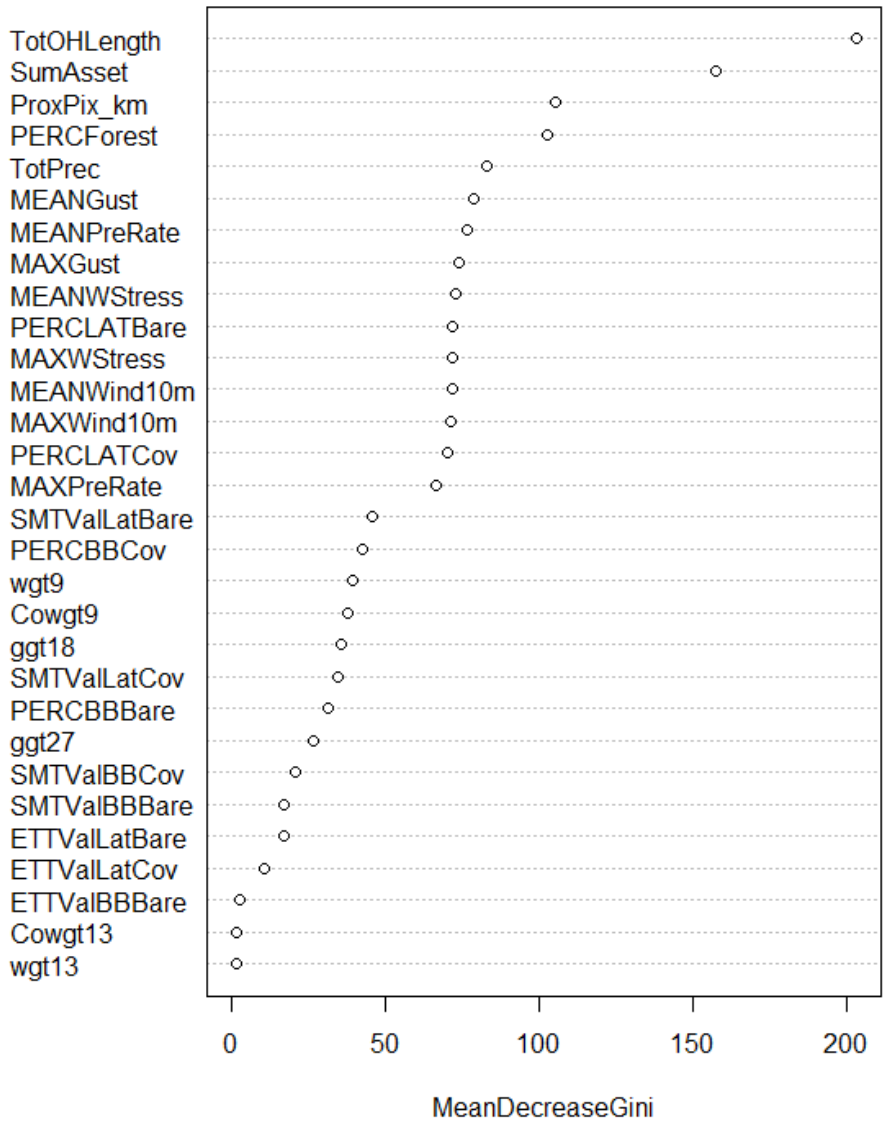

515

516 **Figure 6:** Variable importance plot from Model 5.

517

518

519

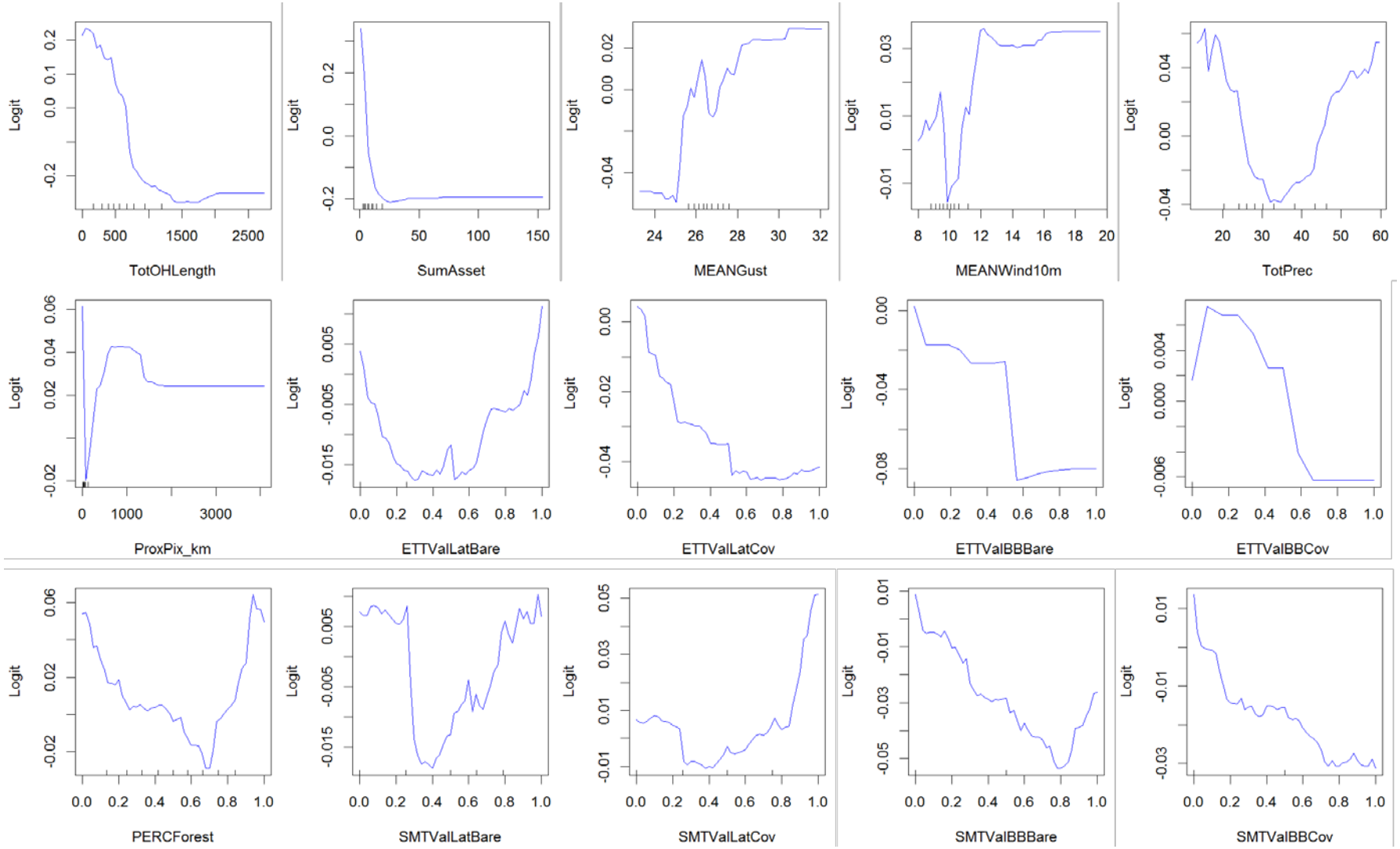

520

521 **Figure 7:** Partial dependence plots from Model 5 for select covariates. See Table I for a list of abbreviations.

522 **Table I:** List of variables included in models. Asterisk (*) denotes maximum and mean variables calculated.

Variable	Abbreviation	Description	Type	Units	Model 1	Model 2	Model 3	Model 4	Model 5
Duration of wind at 10 meters above 9 m/s	wgt9	Weather	Continuous	hr	X	X	X	X	X
Duration of wind at 10 meters above 13 m/s	wgt13	Weather	Continuous	hr	X	X	X	X	X
Duration of wind at 10 meters above 18 m/s	wgt18	Weather	Continuous	hr	X	X	X	X	X
Continuous duration of wind at 10 meters above 9 m/s	cowgt9	Weather	Continuous	hr	X	X	X	X	X
Continuous duration of wind at 10 meters above 13 m/s	cowgt13	Weather	Continuous	hr	X	X	X	X	X
Continuous duration of wind at 10 meters above 18 m/s	cowgt18	Weather	Continuous	hr	X	X	X	X	X
Duration of wind gusts above 18 m/s	ggt18	Weather	Continuous	hr	X	X	X	X	X
Duration of wind gusts above 27 m/s	ggt27	Weather	Continuous	hr	X	X	X	X	X
Duration of wind gusts above 36 m/s	ggt36	Weather	Continuous	hr	X	X	X	X	X
Duration of wind gusts above 45 m/s	ggt45	Weather	Continuous	hr	X	X	X	X	X
Total accumulated precipitation	TotPrec	Weather	Continuous	mm	X	X	X	X	X
Wind stress*	WStress	Weather	Continuous	unitless	X	X	X	X	X
Wind gust*	Gust	Weather	Continuous	m/s	X	X	X	X	X
Wind at 10 m height*	Wind10m	Weather	Continuous	m/s	X	X	X	X	X
Precipitation Rate*	PreRate	Weather	Continuous	mm/hr	X	X	X	X	X
Sum of Assets	SumAsset	Infrastructure	Continuous	count	X	X	X	X	X
Total Length of Overhead Lines	TotOHLength	Infrastructure	Continuous	m	X	X	X	X	X
Percentage Backbone Bare Lines	PercBBBare	Infrastructure	Continuous	m		X	X	X	X
Percentage Backbone Covered Lines	PercBBCov	Infrastructure	Continuous	m		X	X	X	X
Percentage of Lateral Bare Lines	PercLATBare	Infrastructure	Continuous	m		X	X	X	X
Percentage of Lateral Covered Lines	PercLATCov	Infrastructure	Continuous	m		X	X	X	X
Percent Forested	PERCForest	Land Cover	Continuous	%	X	X	X		
Percentage of Backbone Bare - ETT	ETTValBBBare	Vegetation Management	Continuous	%			X		X

Percentage of Lateral Bare – ETT	ETTValLatBare	Vegetation Management	Continuous	%			X		X
Percentage of Lateral Covered - ETT	ETTValBBCov	Vegetation Management	Continuous	%			X		X
Percentage of Lateral Covered - ETT	ETTValLatCov	Vegetation Management	Continuous	%			X		X
Percentage of Backbone Bare - SMT	SMTValBBBare	Vegetation Management	Continuous	%			X		X
Percentage of Lateral Bare – SMT	SMTValLatBare	Vegetation Management	Continuous	%			X		X
Percentage of Lateral Covered - SMT	SMTValBBCov	Vegetation Management	Continuous	%			X		X
Percentage of Lateral Covered - SMT	SMTValLatCov	Vegetation Management	Continuous	%			X		X
ProxPix per kilometer	ProxPix_km	Hazardous Tree Pixels	Continuous	ProxPix/km				X	X

Table II: Counts of which model was the winner using repeated balanced sampling.

Model	AUC	FOR	TPR	TNR	PC	K
Model 1	658	477	477	2475	658	658
Model 2	1530	1486	1486	1833	1530	1530
Model 3	1646	1754	1754	1700	1646	1646
Model 4	**3706**	3118	3118	**2486**	**3706**	**3706**
Model 5	2460	**3165**	**3165**	1506	2460	2460

Table III: Relative improvement in the error metrics compared to baseline model (Model 1)

Model	AUC	FOR	TPR	TNR	PC	K
Model 1	-	-	-	-	-	-
Model 2	132.5%	211.5%	211.5%	-25.9%	132.5%	132.5%
Model 3	150.2%	267.7%	267.7%	-31.3%	150.2%	150.2%
Model 4	**463.2%**	553.7%	553.7%	**0.4%**	**463.2%**	**463.2%**
Model 5	273.9%	**563.5%**	**563.5%**	-39.2%	273.9%	273.9%

Table IV: Selecting the best model overall using the ranking scheme

Model	Rank(AUC)	Rank(FOR)	Rank(TPR)	Rank(TNR)	Rank(PC)	Rank(K)	Average Rank	Final Rank
Model 1	5	5	5	2	5	5	4.5	5
Model 2	4	4	4	3	4	4	3.8	4
Model 3	3	3	3	4	3	3	3.2	3
Model 4	**1**	2	2	**1**	**1**	**1**	**1.3**	**1**
Model 5	2	**1**	**1**	5	2	2	2.2	2